Once-Per-Step Control of Ankle Push-Off Work Improves Balance in a Three-Dimensional Simulation of Bipedal Walking

Myunghee Kim and Steven H. Collins

***Abstract*—Individuals with lower limb amputation have a high fall risk, which could be partially due to a lack of stabilizing control in conventional prostheses. Inspired by walking robots, we hypothesized that modulating prosthetic ankle push-off could help improve amputee balance. We developed a three-dimensional walking model, found limit cycles at two speeds, and designed state-feedback controllers that made once-per-step adjustments to ankle push-off work, fore-aft and medial-lateral foot placement, and ankle roll resistance. To assess balance, we applied increasing levels of random changes in ground height and lateral impulses until the model fell down within 100 steps. Although foot placement is known to be important for balance, we found that push-off control was at least twice as effective at recovering from both disturbances at both speeds. Push-off work affected both fore-aft and mediolateral motions, leading to good controllability, and was particularly well suited to recovery from steps up or down. Our results suggest that discrete control of ankle push-off may be more important than previously thought, and may guide the design of robotic prostheses that improve balance.**

***Index Terms*—Biomechanics, human performance augmentation, legged robotics, rehabilitation robotics, stability.**

I. Introduction

INDIVIDUALS with below-knee amputations experience increased fall rates and reduced balance confidence [1], which reduces mobility and can cause avoidance of social activity [2]. Prior research has established a connection between falling and reduced stability [3]–[6] and has shown that training amputees in recovery strategies can reduce fall risk [7]–[9]. Robotic lower limb prostheses might also prevent falls by improving stability during walking, although most development efforts have focused on other aspects of gait such as average joint kinematics or energy use [10]–[13]. Stability-related outcomes have been compared across devices in some cases [14]–[16], but results have been inconclusive.

The best understood methods for stabilizing gait involve control of foot placement and center of pressure, but these are difficult to implement in robotic ankle–foot prostheses. Simple models of walking suggest that foot placement is an efficient approach to balance, since small adjustments prior to heel strike can have large effects on the trajectory of the ensuing step [17]. This phenomenon is central to "capture point control," which is used for disturbance recovery in humanoid robots [18]. Experimental studies with nonamputee subjects [19], [20] and individuals with below-knee amputation [15] suggest that humans use a similar approach during walking. In humanoid robotics, control of the center of pressure (often referred to as the "zero moment point") between the foot and the ground has also been central to many stable walking algorithms [21]. Humans also seem to modulate the center of pressure location for balance to some degree [22], and individuals with above-knee amputations to exhibit increased reliance on this strategy in the intact limb [23]. These two control approaches are strongly linked; foot placement constrains the region of possible center of pressure locations and defines the location corresponding to zero ankle torque, while center of pressure adjustment through ankle activity is akin to slightly moving the foot after contact has been established. Although these forms of control can be effective and seem to be commonly used for balance by humans, they would be difficult to implement with a robotic ankle prosthesis. Foot placement control is most easily achieved through hip actuation, while center of pressure control is most effective using a wide, flat foot with multiple actuated degrees of freedom, neither of which are currently available in lower limb prostheses.

Ankle push-off work modulation is a promising alternative stabilization method. Regulating system energy is necessary for stable locomotion and simple two-dimensional (2-D) models of gait show that system energy can be strongly affected by the magnitude of work produced by active plantar flexion of the trailing ankle during transitions between steps [24]. Modulation of this ankle "push-off," in concert with control of foot placement, has been used to stabilize simple 2-D walking robots [25], [26]. Three-dimensional (3-D) walking seems to be less stable, however, with the least stable modes corresponding to

Manuscript received May 19, 2016; revised September 2, 2016; accepted November 7, 2016. Date of publication January 16, 2017; date of current version April 3, 2017. This paper was recommended for publication by Associate Editor A. Ude and Editor A. Kheddar upon evaluation of the reviewers' comments. This work was supported in part by the National Science Foundation under Grant CMMI-1300804 and Grant IIS-1355716 and in part by the National Institutes of Health under Award 1R43HD076518-01. This work used the Extreme Science and Engineering Discovery Environment (XSEDE), which was supported by the National Science Foundation under Grant ACI-1053575. *(Corresponding author: Steven H. Collins.)*

M. Kim is with the Department of Mechanical Engineering, Carnegie Mellon University, Pittsburgh, PA 15213 USA (e-mail: myunghek@andrew.cmu.edu).

S. H. Collins is with the Department of Mechanical Engineering and the Robotics Institute, Carnegie Mellon University, Pittsburgh, PA 15213 USA (e-mail: stevecollins@cmu.edu).

This paper has supplementary downloadable material available at http://ieeexplore.ieee.org.

Color versions of one or more of the figures in this paper are available online at http://ieeexplore.ieee.org

Digital Object Identifier 10.1109/TRO.2016.2636297

1552-3098 © 2017 IEEE. Personal use is permitted, but republication/redistribution requires IEEE permission.
See http://www.ieee.org/publications_standards/publications/rights/index.html for more information.

mediolateral motions [17]. Push-off work modulation might still be effective in such systems if ankle push-off were to have some control authority over mediolateral motion of the body. If ankle push-off control were found to be effective at stabilizing 3-D walking, it would help us to explain balance deficits in individuals with amputation below the hip of the affected limb. It would also be feasible to implement push-off modulation in active ankle–foot prostheses, which could improve balance for millions of individuals with lower limb amputation.

Simulations of limit cycle walking could provide well-controlled comparisons of the effectiveness of push-off work, foot placement, and center of pressure control techniques. Limit cycle models can capture features of the basic dynamics of human gait, while remaining simple enough to be intellectually accessible. Such models seem to help explain, for example, how step length [27] and foot shape [28] relate to energy use or why crouch gait is typically accompanied by stiff-knee gait [29]. Simulation models are especially useful for the study of stability, where they allow a level of precision and control that can be difficult to achieve experimentally. They have previously been used to illustrate the utility of active foot placement as a means of stabilizing 3-D walking [17], with results that are qualitatively consistent with those from experiments in humans [19], [20], [30]. Limit cycle models have also been used to design push-off work controllers for 2-D walking robots [26], resulting in a machine that set the distance record for legged robots [25]. A comparison of these control techniques with 3-D models of gait is therefore likely to provide useful qualitative insights into their strengths and weaknesses, and could lead to the design of improved prosthesis controllers.

The most meaningful measure of stability in this context seems to be the maximum random disturbance that can be tolerated without falling. Many other candidate metrics exist, but do not seem well correlated with the likelihood of falling under real-world conditions [31]. Maximum Floquet multipliers are easily obtained by linearizing a dynamic system around a fixed point, but moderate disturbances often move the system outside the linear region for which they are relevant. Basins of attraction capture behavior in full nonlinear regions, but do not include information about which directions in state space are likely to be encountered, making interpretation difficult. Gait sensitivity norms [32] measure a combination of convergence rate and performance during convergence, but rely on a gait indicator that must be calibrated against a more meaningful measure of stability. Maximum allowable disturbance approaches have none of these issues; they include nonlinear behavior, implicitly capture the relevance of state error direction, and need not be calibrated against additional measures. Maximum allowable disturbance is calculated by selecting a disturbance relevant to real-world falls, such as ground irregularity [33] or lateral pushes [30], and gradually increasing the magnitude of the disturbance until the system can no longer recover. A disturbance should be applied on every step so as to penalize solutions that recover slowly and are therefore susceptible to multiple consecutive disturbances. This means many walking steps must be simulated to evaluate each controller. Simulating more steps increases accuracy but also increases computational cost, and so a minimum acceptable number of steps must be chosen carefully.

Walking speed can also affect stability, and might interact with disturbance recovery strategy. Walking speed is correlated with changes in gait pattern [34], fall risk [35], and ability to recover from some types of disturbances [36]. Considering different disturbances at different walking speeds would therefore lend insight into the conditions under which one or another recovery method is likely to be most effective.

In addition to maximum disturbance rejection, the energy required to balance at submaximal disturbance levels can differentiate control strategies. Active balance during walking seems to require the expenditure of meaningful amounts of metabolic energy in humans [30], [37], which increases in the presence of sensory manipulation or ground-height disturbances [19], [38]. Qualitative differences in energy requirements across control strategies could also be explored in simulation.

Simple, low-order control strategies are preferable when transferring controllers from a simulation to hardware because they tend to result in better robustness against errors in the model and to rely on less sensor information. In simulation, full-state linear feedback controllers, e.g., derived as linear quadratic regulators (LQRs), are likely to result in effective disturbance rejection. Performance for a nonlinear system can be further improved by using numerical optimization of the feedback gain matrix, for example using a covariance matrix adaptation evolutionary strategy (CMA-ES). Simulation models of human walking are likely to differ from the real system, however, meaning that control strategies that depend on complex, accurate models are unlikely to translate well. Controllers based on basic aspects of the system's dynamics are more likely to be successful in humans. Measuring some human states can also be difficult in practice, meaning that some of the information used by a full-state-feedback controller would be unavailable in a real prosthesis. Controllers that only use local state information are therefore more desirable for prosthesis design. Often, full-state-feedback control can be approximated by a simpler controller with similar performance [39], [40].

This simulation study was designed to compare the effectiveness of ankle push-off control against foot placement and ankle inversion–eversion control in 3-D walking. We hypothesized that ankle push-off control could result in similar maximum tolerable disturbances and energy consumption as these more widely used strategies, while relying only upon actuation available to a prosthetic ankle. We also hypothesized that it would be possible to derive a simple, robust form of the ankle push-off controller suitable for use in hardware experiments.

We explored some of these ideas in a preliminary study by using a simpler model and controller, which was presented at ICORR in 2013 [41]. We substantially expand upon these results in this study. We make comparisons of models that walk at both slow and normal speeds and are subjected to both ground-height and lateral-impulse disturbances. We develop new controllers that have been optimized for disturbance tolerance by using an evolutionary strategy for each combination of control input, speed, and disturbance. We have additionally investigated the effects of control type on energy use. Finally, we developed reduced-order controllers suitable for implementation in prosthetic foot hardware.

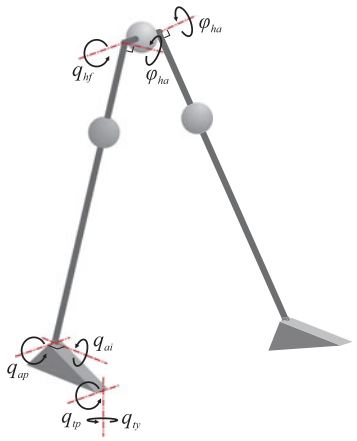

Fig. 1. Model schematic. The model had a finite-width pelvis, two straight legs, and two massless feet. The hip had a flexion–extension joint (q_{hf}), and an abduction angle that could be changed once per step at mid-stance (ϕ_{ha}). The ankle of the stance leg had a plantarflexion joint (q_{ap}) and an inversion (roll) joint (q_{ai}). The stance foot was connected to the ground either rigidly, through a toe pitch joint (q_{tp}), or through both a toe pitch and a toe yaw joint (q_{ty}), depending on phase of the gait cycle. All degrees of freedom are defined such that, beginning at the ground, positive rotation causes the subsequent segment to move in the direction indicated by the arrow.

II. Methods

We developed a 3-D limit cycle walking model with hip and ankle actuation and used it to compare the capacity of foot placement, ankle inversion–eversion control, and push-off work control to stabilize gait against ground-height disturbances and lateral-impulse disturbances. The model has finite pelvis width, two straight legs attached to the pelvis via hip joints, and massless feet connected to the legs via ankle joints. Hip joints were controlled to modulate step length and step width, while ankle joints were controlled to change ankle roll resistance and ankle push-off work. After developing nominal controllers for the hip and ankle joints, corresponding to two gait speeds, we designed discrete stabilizing controllers that modulated step length, step width, ankle roll resistance, and ankle push-off work once per step. We compared the performance of each controller in terms of maximum tolerable random disturbance in ground height and lateral impulse. Finally, we developed a hardware-implementable version of the ankle push-off controller and compared its performance with the full state feedback controller.

A. Model

1) Mathematical Model Description: We developed a 3-D walking model with a pelvis, two straight legs, and two feet (Fig. 1). The pelvis and legs were connected via hip joints that allowed continuous flexion-extension and once-per-step changes in adduction-abduction angle (as in [17]). The legs and feet were connected via ankle joints that allowed both plantarflexion–dorsiflexion and inversion–eversion. The inversion–eversion degree of freedom makes this system 3-D, allowing it to fall side to side as well as forwards and backwards. The feet and ground were connected either rigidly, by a toe pitch joint, or by both a toe pitch joint, and a toe yaw joint, depending on phase of stance.

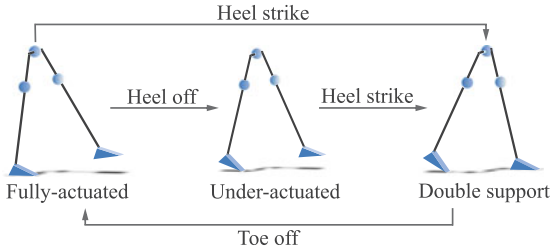

Fig. 2. Model gait phases. During a walking step, the model went through at least two of three possible phases: fully actuated single support, underactuated single support, and double support. From the fully actuated phase, the model could transition to either double support, if foot strike was detected, or to under-actuated single support, if stance heel rise was detected. From the under-actuated phase, the model transitioned to double support when the swing foot touched the ground. From the double support phase, the model transitioned to fully actuated single support when the ground reaction force at the toe of the stance foot became zero.

Mechanical parameters of the model were based on human anthropometrics [42], [43]. Hip width was 0.3 m and leg length was 1 m. Foot length from heel to toe was 0.25 m, while the horizontal distance from ankle to toe was 0.19 m, foot height from base to ankle was 0.09 m, and foot width (used to check center of pressure feasibility) was 0.1 m. Nominal step width, set by choice of nominal hip abduction angle, was 0.15 m. The pelvis had a mass of 54 kg, located at its center, and a rotational inertia of 10 kg·m^2, which together approximated the mass properties of the head, arms, and torso. Each leg had a mass of 10 kg, with center of mass located 0.3 m from the hip joint. The feet were treated as massless

2) Dynamics: During each walking step, the model went through a double support phase, a fully actuated single support phase, and, on most steps, an underactuated single support phase. During double support (Fig. 2) the leading foot was rigidly attached to the ground, while the trailing toe was connected to the ground through a two degree of freedom joint that allowed both pitch and yaw rotations. The yaw degree of freedom gave the closed-loop kinematic chain two degrees of freedom, resulting in more natural motions during double support. Toe off occurred when the vertical component of the reaction force of the trailing toe went to zero, leading to single support. During the initial portion of single support, the stance foot was fixed to the ground, allowing full actuation of the resulting three degrees of freedom (two at the stance ankle and one at the hip). Heel rise occurred when the vertical component of the reaction force of the heel of the stance foot went to zero, leading to the underactuated phase. During the under-actuated phase of single support, the foot was connected to the ground through a hinge joint that allowed pitch rotation, with four degrees of freedom in total. Foot strike was detected when the base of the swing foot reached ground height, after which the model underwent a perfectly inelastic collision and transitioned into double support. On most steps foot strike occurred during the underactuated phase of single support, but with large disturbances foot strike sometimes occurred during the fully actuated phase of single support.

Equations of motion for each phase were obtained by using the Dynamics Workbench [44], a software program based on Kane's method. State trajectories for each step were calculated

by using forward numerical integration. The heel strike collision was modeled using an impulse-momentum approach, in which postcollision velocities were obtained as a function of precollision states. We modeled the body as an open kinematic chain during this collision, and solved for the impulse on the leading foot that would cause it to have zero velocity following the collision. We simultaneously solved for the postcollision velocities of the trailing toe joints, ankle plantarflexion and inversion–eversion joints, and hip flexion joint by performing an angular momentum balance about each joint that included the effect of the impulse on the leading foot.

Limit cycles were found using a gradient search algorithm that altered initial conditions to minimize error between the initial and final states of a walking step. Limit cycles were found at two human-like speeds and step lengths, 1.00 m·s^{-1} with 0.63 m steps and 1.25 m·s with 0.70 m steps, approximating the range of preferred speeds and step lengths of high-activity individuals with lower limb amputation [45]. Limit cycles with desired characteristics were found by using a nested gradient search approach that altered nominal target step length and push-off work to minimize error between the desired and observed speed and step length [46].

B. Actuation and Control

Hip and ankle joints were controlled in two layers: a continuous low-level controller achieved target values of step length, step width, ankle roll resistance, and ankle push-off, while a discrete high-level controller set these targets once per step (Fig. 3).

1) Low-Level, Within-Step Control: Hip flexion-extension torque was continuously controlled to achieve desired step length. We used proportional-derivative control of hip flexion angle, where the set point was ϕ_{hf} and the nominal value corresponded to the preferred step length for humans. We chose relatively high stiffness and damping gains, such that the hip flexion controller settled at target step length within 90% of the stance period at the limit cycle. This resulted in improved fore-aft stability [47].

Hip abduction-adduction angles were set once per step to achieve desired step width. We discretely changed the rigid hip abduction angle paramter ϕ_{ha} at mid-stance in the manner of [17]. The nominal value of ϕ_{ha} corresponded to the preferred step width for human walking.

Ankle inversion–eversion torque was continuously controlled to provide desired levels of resistance. Inversion–eversion torques followed a proportional-derivative control law, with gains of K_p and K_d and set point angle and angular velocity of θ_0 and $\dot{\theta}_0$. The nominal values for K_p and K_d were both zero, and the nominal values of θ_0 and $\dot{\theta}_0$ corresponded to the value of eversion angle and angular velocity just after heel strike during limit cycle motions.

Ankle plantarflexion torque was continuously controlled to provide desired levels of ankle push-off work. Torque was applied as a function of ankle angle and direction of motion, as depicted in Fig. 3(e), or as

$$\tau = -k_{\text{ank}}(\theta - \theta_0) + \max(0, \text{sign}(\dot{\theta})) \cdot \tau_p \qquad (1)$$

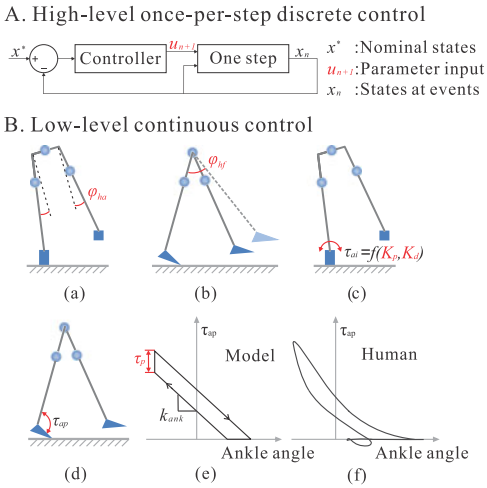

Fig. 3. Control architecture. Control was performed in two layers: (A) high-level, discrete control that used linear state feedback to make adjustments to low-level parameters once per step, and (B) low-level control that continually regulated joint torques in accordance with parameters during the course of a step. The actuation parameters used in low-level control were: (a) hip abduction angle ϕ_{ha} a fixed parameter only changed at mid-stance, which affected step width, (b) target hip flexion angle ϕ_{hf} the set point in a proportional–derivative controller on hip flexion torque, which affected step length, (c) ankle inversion–eversion stiffness K_p and damping K_d gains in a proportional–derivative controller on ankle inversion–eversion torque, which affected roll resistance and medial-lateral center of pressure location, and (d-e) ankle plantarflexion torque offset, τ_p, an offset in ankle torque during the phase when joint velocity was positive, which affected ankle push-off work. (f) Default values of torque offset and ankle stiffness were chosen to approximate the torque-angle curve observed for humans [48].

where τ is ankle plantarflexion torque, k_{ank} is ankle stiffness, θ is ankle plantarflexion angle, θ_0 is nominal ankle angle, $\dot{\theta}$ is ankle angular velocity, and τ_p is the plantarflexion torque offset. The values of k_{ank} and θ_0 were selected so as to approximate the average torque-angle curve of the human ankle, while the nominal value of τ_p was set during the search for a limit cycle with the desired speed and step length. The curve formed by this function in angle-torque space is a work loop, with the area inside corresponding to net ankle work during a step. Because peak dorsiflexion angle is relatively consistent, τ_p is approximately proportional to net ankle work.

2) High-Level, Once-Per-Step Control: We developed several high-level controllers that altered target values of step length, step width, ankle roll resistance, ankle push-off work, or combinations of these low-level control parameters once per step in order to maintain balance. The system was discretized by sampling states once per step at a Poincaré section, or a predefined state event. Each high-level controller was discrete and linear, having the form

$$u_{n+1} = u^* - K(x_n - x^*) \qquad (2)$$

where u_{n+1} is a vector of control inputs (some combination of ϕ_{hf}, ϕ_{ha}, K_p, K_d or τ_p) for the n+1th step, u^* is the nominal vector of control inputs corresponding to limit cycle motion, K is the gain matrix of the discrete linear controller, x_n is the state vector at the end of the nth step, and x^* is the state vector corresponding to limit cycle motions. For most high-level

controllers, we used full state feedback, consisting of the angles and angular velocities of all model joints.

High-level control decisions were made at mid-stance for step length and step width control, and at the instant following heel strike for ankle roll and push-off control. At mid-stance, velocities and displacements of the center of mass were well captured, while sufficient time remained to place the swing foot [25]. At heel strike, control decisions could be implemented immediately in either the trailing or leading ankle.

We developed discrete linear approximations of the dynamics of the model and control inputs and used these to generate feedback gain matrices with an LQR approach. We approximated the discrete dynamics as $x_{n+1} = A \cdot x_n + B \cdot u_n$, where x_{n+1} is the state at the end of the n+1th step, A is the state transition matrix, x_n is the state at the end of the nth step, B is the control input matrix, and u_n is the control input on step n, all relative to nominal values at the fixed point. We used a finite differencing approach to obtain the A matrix and B matrices corresponding to each set of control inputs. These models were then used to generate LQRs, each consisting of a gain matrix K for use in (2). A finite differencing approach was also used to calculate linear approximations of other aspects of system dynamics, such as the effects of disturbances on system states, to aid interpretation of results.

We found that disturbance rejection could be significantly improved by refining the gain matrix using a genetic algorithm. This improvement likely relates to the fact that the LQR result is optimal only in a narrow linear region, and does not utilize information about the types of disturbances likely to be encountered. The value of K determined using LQR was used as an initial seed in a CMA-ES optimization [49]. We used the cost function $f = 1/h$, where h was the maximum tolerable disturbance for the full nonlinear system. We used a population size of 30 to minimize computation time. The algorithm typically underwent 150 to 300 generations before convergence. This process was repeated for each combination of control input, disturbance, and gait speed (requiring the simulation of hundreds of millions of walking steps). The resulting optimized gain matrices were used in across-controller comparisons.

C. Stability Measure

We quantified stability as the maximum random floor height disturbance and the maximum random lateral-impulse disturbance that the model could tolerate for 100 steps without falling. Before each walking bout, bounded, evenly distributed, random arrays of floor heights and impulses (Fig. 4) were generated. The magnitude of the floor height disturbance was defined as the difference between the upper and lower bounds of possible floor heights. The magnitude of lateral-impulse disturbance was defined as the absolute value of the largest possible impulse, which could be applied in either direction. Impulses were applied at the instant of heel strike on each step. Maximum tolerable disturbance was found by slowly increasing the magnitude until the model was unable to complete a predefined number of steps without falling.

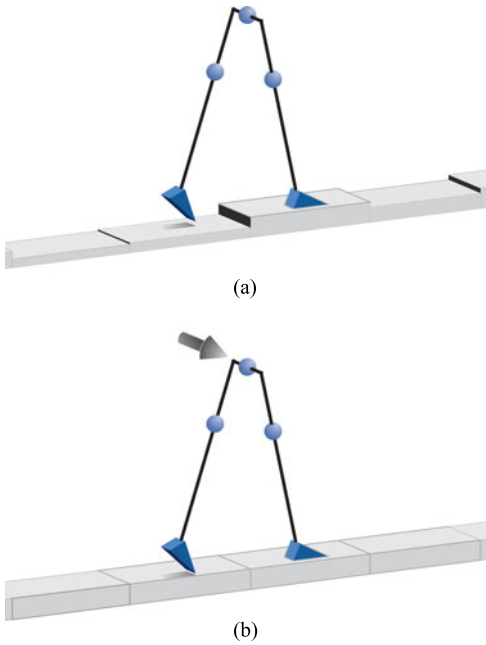

Fig. 4. Disturbances in (a) ground height and (b) lateral impulse. The ground was modeled as a series of flat surfaces, each centered below the landing foot, and each with a randomly chosen height with respect to a constant reference. Possible tripping of the swing foot was not considered. The magnitude of the disturbance was defined as the maximum possible change in height between two consecutive steps. Lateral disturbances were applied as an impulse along the main axis of the pelvis at the instant of heel strike on each step.

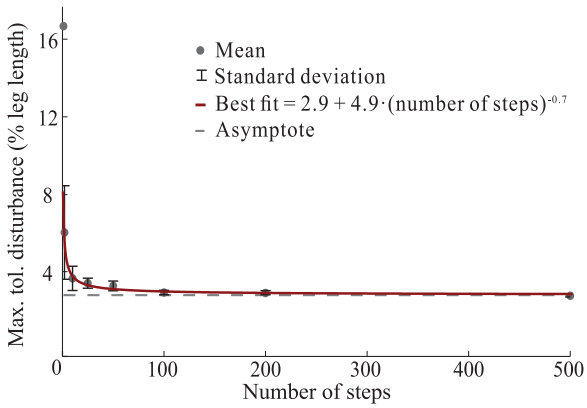

Fig. 5. Maximum tolerable ground-height disturbance versus number of steps tested. Dots and whiskers are the means and standard deviations of five tests of maximum allowable disturbance using different random ground patterns. We fit data with an exponential curve, shown in red. The mean approached a constant as the number of steps increased, shown as a dashed line, while standard deviation approached zero. At 100 steps, the mean maximum tolerable disturbance value was within 2% of the asymptote.

To determine an appropriate number of steps, we tried several values and compared disturbance tolerance. We generated five sets each of random height distributions having lengths from 1 to 500 steps, and calculated the mean and standard deviation of maximum tolerable disturbance at each length (Fig. 5). We found that maximum tolerable disturbance appeared to converge to within 2% of the final value when at least 100 walking steps were tested, and that the standard deviation across different

randomly generated ground patterns was also less than 2% for this number of steps. We therefore used 100 continuous steps in tests of disturbance tolerance.

D. Energy Expenditure Measure

We used positive mechanical work performed by hip and ankle joints to quantify energy use. This system is periodic and does not, on average, change speed or height. Positive and negative mechanical work are therefore equal and opposite on average, with positive joint work replacing negative joint work and dissipation in plastic collisions. We calculated energy use for submaximal disturbance levels, ranging from no disturbance to maximum tolerable disturbance, in order to capture changes in energy consumption associated with balance.

E. Hardware-Implementable Control

For the most effective full-state-feedback controllers, we developed reduced-order versions suitable for implementation in robotic prosthesis hardware. Sensory information was limited to local measurements only, including step period and ankle joint angles and velocities. We first used linear regression to calculate new gain matrices that used reduced sensory information to reproduce the full-state-feedback control inputs with least-squared error. These gains were refined for the nonlinear system by using a genetic algorithm (CMA-ES).

F. Simulation Experiment

We compared disturbance tolerance among the most effective high-level controllers. In particular, we compared controllers based on step length and step width (foot placement), ankle stiffness and damping (ankle roll resistance), (both stiffness and damping), ankle push-off work, and the combination of all five control inputs. For the normal walking speed model, we compared energy use across controllers, and compared full-state-feedback controllers with their reduced-order hardware-implementable analogues.

III. Results

Once-per-step control of ankle push-off work resulted in better disturbance rejection than control of foot placement or ankle roll resistance for both disturbance types and gait speeds. Performance with push-off work control alone was nearly as effective as controlling all inputs together (Fig. 6). Push-off work modulation allowed the model to withstand random changes in ground height of up to 7.8% of leg length (0.085 m) compared to 1.5% leg length (0.016 m) with foot placement, or about five times greater disturbance tolerance, at a normal walking speed. The push-off controller tolerated random lateral disturbances of up to ±6.3 N·s, compared to ±2.6 N·s with foot placement, or about twice the disturbance tolerance. For larger disturbances, the push-off controller failed to achieve ground clearance with the swing foot in at least one step in 100. For foot placement and ankle roll resistance controllers, the model fell sideways with higher disturbances, consistent with prior modeling results [17].

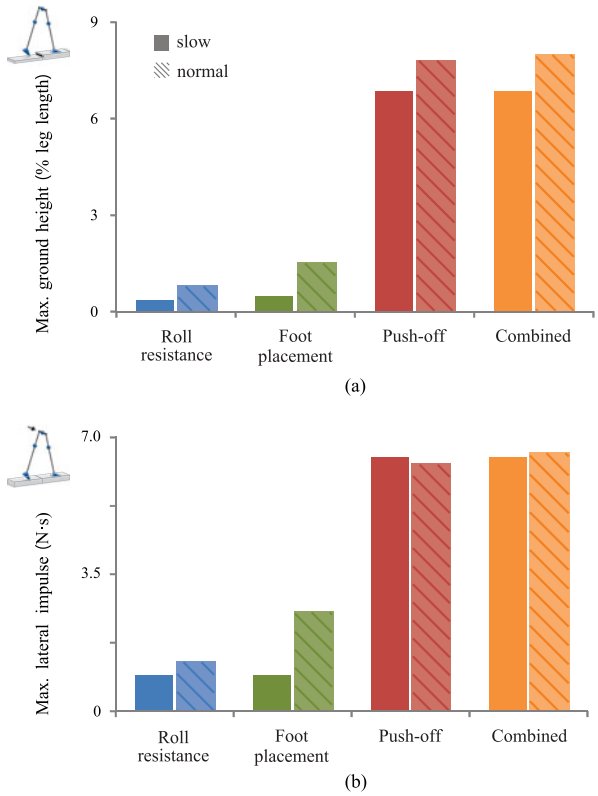

Fig. 6. Disturbance tolerance versus control approach. (a) Maximum tolerable ground-height disturbance. (b) Maximum tolerable lateral impulse. Bars represent the maximum, bounded, random, ground-height variation, and maximum absolute value of bounded, random, bidirectional, lateral impulse that the model could tolerate for 100 steps without falling. Solid bars are for slow walking (1.0 m·s) and patterned bars are for normal walking (1.25 m·s). Four different high-level controllers were tested: foot placement, based on ϕ_{ha} and ϕ_{hf}; ankle roll resistance, based on K_p and K_d; ankle push-off work, based on τ_p; and combined, based on ϕ_{ha}, ϕ_{hf}, K_p, K_d, and τ_p. Ankle push-off work control led to the greatest disturbance tolerance.

Optimization of gain matrices using a genetic algorithm improved disturbance tolerance for all controllers, but did not affect the trend across controllers. For example, maximum tolerable disturbances using the unmodified gain matrices derived with LQR were 2.9% and 1.0% of leg length using push-off work control and step width control, respectively, at the normal walking speed. A full comparison of results for the two design methods is provided in the Appendix.

Other candidate measures of stability, including maximum Floquet multiplier and gait sensitivity norm, did not correlate well with maximum tolerable random disturbance (although push-off control was effective by these measures). A comparison of stability metrics is provided in the Appendix.

In the linearized model, ankle push-off had strong control authority over both mediolateral and fore-aft motions. This is illustrated by the normalized, weighted effects of each input on the three states primarily associated with center-of-mass position and velocity at mid-stance (Table I; detailed calculation in Appendix). At mid-stance, defined as the instant the hip passed over the ankle ($q_{\mathrm{ap}} = 0$), push-off (τ_p) strongly affected lateral center-of-mass position (q_{ai}) and both fore-aft and lateral center-of-mass velocities ($\dot{q}_{\mathrm{ap}}$ and $\dot{q}_{\mathrm{ai}}$). Increased push-off work

TABLE I
NORMALIZED CENTER-OF-MASS STATE CHANGES AT MID-STANCE

		Control input					Disturbance	
		K_p	K_d	ϕ_{ha}	ϕ_{hf}	τ_p	Ht	Imp
State	q_{ai}	−0.941	−0.822	−0.982	−0.929	0.634	−0.600	0.951
	$\dot{q}_{\text{ap}}$	−0.013	−0.013	−0.045	0.219	−0.715	0.752	0.016
	$\dot{q}_{\text{ai}}$	−0.337	−0.569	−0.185	−0.299	0.295	−0.273	0.310

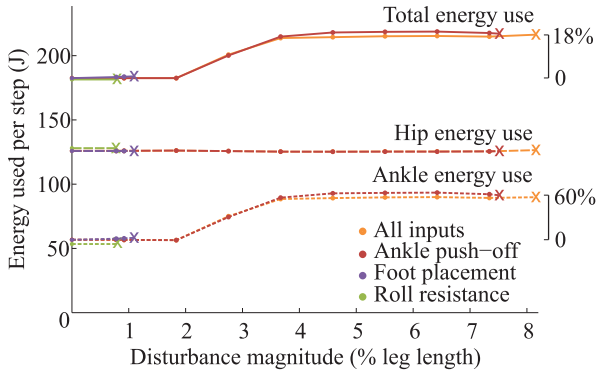

Fig. 7. Energy expenditure of the normal speed model under the ground-height disturbances as a function of disturbance magnitude. Solid lines represent total energy use, long-dashed lines the component used at the hip and short-dashed lines the component used by the ankle. Colors represent different high-level controllers, with X's indicating the point at which the model could no longer tolerate disturbances. Energy used at the hip was unchanged with increasing disturbance. Ankle energy use increased in the region between about 2% and 4% of leg length, corresponding with an increase in walking speed and a shift to a gait pattern in which the model tended to transition into double support without heel rise in the stance foot.

led to lateral displacement of the center of mass and increases in both lateral and forward center-of-mass velocity at mid-stance. These effects were nearly equal and opposite to those caused by a step up in ground height (Ht). Step length (ϕ_{hf}) had a similar set of effects on center-of-mass mechanics, but with less weight on forward velocity. Ankle inversion resistance and step width (K_p, K_d, and ϕ_{ha}) had little effect on fore-aft motion, but were well aligned with the effects of lateral impulses (Imp). Center-of-mass state was controllable through any input, but push-off led to the best conditioned controllability matrix. The effects of push-off on center-of-mass state were linear over a large region ($\tau_p > 100$ N·m) compared to the linear regions for other inputs such as step width ($\phi_{\text{ha}} \leq 0.04$ rad). The Appendix includes a more detailed explanation, including comparisons of input-disturbance alignment, controllability, and linearity.

Energy use did not correlate with disturbance magnitude. For all high-level controllers, changes in positive joint work were negligible for low levels of ground-height disturbance (below 1% leg length; Fig. 7). In this region, step-by-step differences in energy use due to control actions canceled out over many steps. At higher levels of disturbance only ankle push-off work control was able to maintain balance, and energy use increased due to a change in walking speed. As disturbance magnitude increased from around 2% to 4% leg length, walking speed increased by about 20%, from 1.25 to 1.54 m·s. This change in speed arose through dynamic interactions between the disturbance, resulting state errors, the optimized gain matrix, and resulting ankle push-off work. At higher speeds, trailing ankle stiffness k_{ank} was too low to cause the stance heel to rise prior to leading leg collision. This led to a sharp increase in the prevalence of steps in which heel rise did not occur prior to heel strike, from 0% of steps with 2% leg length disturbances to more than 90% of steps with 4% leg length disturbances. With the stance foot flat on the ground prior to heel strike, the center of mass velocity was directed more downwards, leading to greater energy dissipation in the ensuing collision. Over the same range, overall energy use increased by about 20%, which was entirely accounted for by a 60% increase in positive mechanical work at the ankle joint.

We explored many reduced-order control strategies, and found that reasonable performance could be achieved via push-off control based on sensed ankle inversion–eversion velocity alone. Using linear regression, target push-off work matched that calculated using full-state feedback with about 19.5% root-mean-squared error. After optimization of the gain matrix (in this case $K \in \mathbb{R}^1$) using a genetic algorithm, the reduced-order push-off work controller tolerated ground-height disturbances of 1.8% leg length. This reduced-order feedback law essentially stated that when mediolateral velocity was too low at heel strike, push-off should be increased. More precisely, the controller commanded push-off work in proportion to the difference between the measured and expected ankle inversion velocity

$$\tau_p = \tau_p^* - K \cdot (\dot{q}_{\text{ai}} - \dot{q}_{\text{ai}}^*) \tag{3}$$

where τ_p is the torque offset (proportional to net ankle work), τ_p^* is the nominal torque offset, K is a positive scalar, $\dot{q}_{\text{ai}}$ is measured ankle eversion velocity, related with mediolateral center-of-mass velocity, with positive velocity defined as causing the model to move side-to-side in the direction of the leading leg during double support, and $\dot{q}_{\text{ai}}^*$ is ankle eversion velocity at the fixed point of the limit cycle.

IV. DISCUSSION

We compared the effectiveness of once-per-step control of ankle push-off work, foot placement, and ankle roll resistance at recovering from random disturbances in ground height and lateral impulse. Control of push-off work was by far the most effective approach, tolerating changes in ground height and lateral impulse that were at least two times greater than any other strategy, regardless of the speed of the model. This strongly suggests that ankle push-off work can be an important contributor to balance maintenance in the presence of the types of disturbances expected in human environments.

Although most explanations of the role of ankle push-off have focused on the sagittal plane [50], [51], ankle push-off also has strong control authority over mediolateral motions. Under typical conditions, push-off torque leads to both vertical and mediolateral components of force at the trailing toe (Fig. 8), contributing to side-to-side accelerations of the center of mass. Increased ankle push-off work thereby increases forward, vertical, and lateral center-of-mass velocity, leading to commensurate changes at mid-stance (Table I). This can be used to aid recovery in both sagittal and frontal planes. Push-off work may therefore be more important for maintaining frontal-plane stability than previously thought.

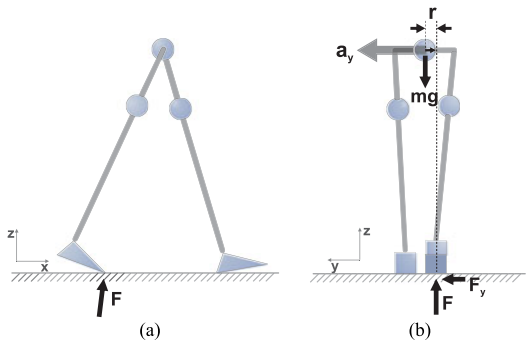

Fig. 8. Push-off affects frontal plane dynamics. The force generated by push-off (F), usually described in (a) the sagittal plane, can also affect (b) frontal plane motions. With finite mediolateral distance between the foot and the center of mass (r), the combined effects of push-off force and body weight lead to a mediolateral force at the foot (F_y) and a mediolateral component of body acceleration (a_y). If one neglects rotational inertia about the center of mass and 3-D coupling, lateral acceleration is proportional to push-off force as $a_y = \frac{1}{m} \cdot \frac{r}{L} \cdot F$, where L is leg length.

Once-per-step control of push-off work may have been more effective at recovery from ground-height disturbances in part because the effects of these two inputs on center-of-mass mechanics were so similar. Increased push-off work led to lateral center-of-mass displacement and increased lateral and forward velocity at mid-stance (Table I). This almost exactly counteracted the effects of a step up, possibly allowing recovery within a single step. No other inputs were as well aligned with ground-height disturbances (Table VII).

Once-per-step control of push-off work seems to have been more effective at recovery from lateral impulses due to better controllability and a larger linear range than other inputs. The effects of lateral impulse on center-of-mass state were best aligned with ankle roll resistance and step width, rather than push-off work. However, push-off resulted in a center-of-mass controllability matrix that was six times better conditioned than ankle roll resistance and sixty times better conditioned than step width (Table VIII). Appropriate sequences of push-off work could thereby achieve various changes in state more easily. For example, an increase in push-off work on one step followed by a decrease in push-off work on the next step has nearly the same effect on center-of-mass state as a lateral impulse; forward velocity is unaffected, while lateral position and velocity are both increased, because side-to-side velocity reverses from step to step while forward velocity does not. The linear range of push-off was also much larger than that of other control inputs. Torque during push-off could be doubled or eliminated with predictable effects, while, for example, step width could only be adjusted by 28% before causing a fall within one step (Table IX). Greater controllability and a greater linear region may also have allowed better regulation of system energy than other inputs. These factors seem to be responsible for the greater disturbance tolerance achieved with push-off work control across all conditions tested.

The simplified push-off controller based on ankle inversion velocity commanded more push-off work when velocity was reduced at the instant of heel strike. An unexpected step up leads to lower side-to-side velocity at heel strike because the swing foot strikes the ground earlier than normal, halting center-of-mass acceleration toward the leading leg. Pushing off more helps us to recover both mediolateral velocity and fore-aft velocity, injecting additional energy needed to vault over the elevated stance leg. In the context of random disturbances in ground height, this simplified control law could be summarized as "if you step on a bump, push off more; if you step in a hole, push off less." An unexpected lateral impulse increases mediolateral velocity, but in this case pushing off less undesirably decreases forward velocity. With the correct choice of gain, however, some of the mediolateral disturbance persists into the next step, this time triggering an increase in push-off work from the controller. The net effect of pushing off less on one step and more on the next is a strong change in mediolateral velocity but not forward velocity. In the context of lateral impulses, the simplified control law could be summarized as "if you get pushed toward your swing leg side, push-off a bit less on this step and a bit more on the next." What is surprising is that the most important effects of modulating push-off, for both disturbances, seem to be on frontal plane dynamics.

Discrete ankle push-off control resulted in the greatest disturbance tolerance for all gait variations and control design approaches that we explored. Push-off control performed better at both slow and normal speeds, with both random ground height and random lateral impulses, and with controllers designed using both LQR and CMA-ES. In a model variant with spring-like hip flexion (described in the Appendix), similar to those used in prior simple dynamic models [52], disturbance tolerance was reduced for all high-level controllers (e.g., 0.7% leg length with push-off control) but had the same trend across controllers (e.g., 0.1% leg length with step width control). In a model variant with larger nominal step width (described in the Appendix), both energy use and maximum tolerable disturbances increased slightly, as reported in previous studies [17], but the relative disturbance tolerance of high-level controllers was the same. The effectiveness of ankle push-off control across all these circumstances suggests that it may be an important contributor to balance in human walking.

In this model, there was no increase in mechanical energy cost associated with control actions to maintain balance in the presence of increasing disturbances. For small disturbances, no change in energy use occurred for any control type. For larger disturbances, push-off control actions tended to increase walking speed, which led to increased nominal energy cost. In optimizing the controller, rejection of errors in the more fall-prone mediolateral direction might have been achieved at the cost of poorer rejection of errors in the fore-aft direction. Increased walking speed might also have been a strategy for improving nominal stability discovered by the genetic algorithm. Whatever the cause, increased energy use at high disturbance levels was not due to step-by-step changes in joint work associated with balance. This bodes well for the application of push-off control in robotic prostheses, since it might not require an increase in average power output.

Although we only considered linear state-feedback controllers, the results reported here are consistent with prior simulation studies utilizing nonlinear control of foot placement or center of pressure. We optimized the gains of our feedback controllers using a genetic algorithm, resulting in substantial

improvements in disturbance tolerance, but did not alter the linear control architecture itself. In general, nonlinear control encompasses a larger design space and is expected to result in better performance. It is possible that disturbance tolerance could be improved more with nonlinear control for approaches using foot placement and center of pressure than those using ankle push-off. To provide context, we repeated tests applied in two previous simulation studies examining stability with nonlinear control and compared outcomes (see Appendix for details). We found that the best foot placement controller derived here tolerated similar maximum downhill slopes as a prior foot placement approach (-2.5° compared to -3° slope in [53]). Similarly, the ankle inversion–eversion resistance controller derived here tolerated a similar step down as a prior center of pressure approach (0.057 m compared to 0.025 m in [54]). These comparisons suggest that the linear controllers used here do not put foot placement or center of pressure techniques at a substantial disadvantage. With the addition of techniques such as LQR trees [55], we would expect improvements in disturbance tolerance for all control inputs. Similarly, the addition of planning for imperfectly anticipated disturbances would likely lead to improvements for all control inputs. A more complete model might also have lent insights into the effectiveness of other balance strategies, such as those using the arms and torso. Both the trunk [56] and arms [57] have been suggested as contributors to stability in human gait, and these should be investigated in future studies.

The finding that ankle push-off work control was more effective than foot placement and ankle roll resistance control may be specific to random ground-height and lateral-impulse disturbances. In particular, random disturbances on each step can result in different relative effectiveness of control inputs than single disturbances. With a single step down, both ankle push-off and foot placement yielded the same disturbance tolerance (8.3% leg length), with the limiting factor being foot clearance on the next step. With a single lateral impulse, ankle roll resistance tolerated 15% larger disturbances than ankle push-off (see Appendix for details). Control inputs with weaker authority may benefit more from the additional recovery time allowed by single disturbances, making continual random disturbances a stronger test of balance. In all cases we have tested, push-off control has resulted in disturbance tolerance that was at least comparable to other inputs.

Control of foot placement and push-off work occurred at different times in the gait cycle, an unavoidable consequence of the nature of these control inputs that can disadvantage foot placement. Disturbances took effect at heel strike. The effects of foot placement control occurred primarily at the next heel strike, by which time the disturbance had substantially affected the full state of the system. Push-off work decisions were made directly after heel strike, at which time only system velocities had been affected. In the discretized linear system such differences do not matter; the characteristic delay is one walking step regardless of the time between the disturbances and control actions within the step. This system, however, is meaningfully nonlinear. Larger disturbances push the state beyond its approximately linear region, illustrated, for example, by the improvements obtained by CMA-ES gain tuning after LQR design. A longer delay between disturbances and corrections can therefore lead to larger state deviations and more nonlinear effects. For ground-height disturbances such timing discrepancies are unavoidable; the disturbance takes effect at heel strike, after which foot placement cannot be adjusted because the foot is already on the ground. Push-off work, by contrast, can still be modulated during the ensuing double-support period. For lateral-impulse disturbances, applying the impulse just before mid-stance might advantage foot placement over push-off work, although this idea remains to be tested.

Delays between control decisions and control actions could also advantage push-off modulation over foot placement in some situations, although not in the present simulation. Foot placement decisions were made at mid-stance, with their primary effects on system dynamics occurring at the subsequent heel strike. If additional disturbances were to occur in the intervening portion of swing, they would not be accounted for in that foot placement. Such delays are inherent in the foot placement strategy, but not in push-off work modulation. Changing leg position with torque- and speed-limited actuators requires finite time, and these delays frequently limit performance in robots with foot placement control strategies [47], [58], [59]. By contrast, altering trailing ankle push-off work requires only a change in ankle torque, which can be achieved much faster. Delays between control decisions and actions were not an issue in this study because additional disturbances did not occur between sensing and action.

As a follow-on to this simulation study, we have recently conducted and published a study demonstrating that once-per-step modulation of push-off work in an ankle–foot prosthesis can improve balance for humans [60]. Our experimental work provides empirical evidence to support the primary finding of the present modeling study, which is that control of push-off work is important to balance for 3-D bipeds.

V. Conclusion

In this study, we have shown that once-per-step control of ankle push-off work can be more effective than foot placement and center of pressure control when recovering from random changes in ground height and random lateral impulses in 3-D bipedal walking. The key to this result seems to be that push-off provides a useful combination of effects on both mediolateral and fore-aft motions. A simplified controller that adjusted push-off based only on ankle inversion–eversion velocity was also effective, correcting reductions in lateral velocity at heel strike by commanding more push-off work, and vice versa. The simplified controller is relatively easy to implement in a prosthesis because it requires only local state information and has only one gain that requires tuning. The technique also requires no additional power on average, meaning that its incorporation in a mobile device would not require larger batteries. The theoretical framework presented here explains our recent success in reducing balance-related effort for humans using once-per-step control of push-off work in an ankle–foot prosthesis. This approach could be utilized in commercial prostheses, possibly leading to devices that improve balance and reduce fall risk for individuals with lower limb amputation.

APPENDIX

A. Gain Optimization

We examined the maximum tolerable disturbances in ground height with once-per-step controllers using two different gain optimization methods, LQR and CMA-ES (Table II). Comparisons were made at normal walking speed. CMA-ES resulted in substantially greater disturbance tolerance for most controllers. The improvement for the foot placement controller was relatively small (0.002% leg length). For both methods of gain generation, ankle push-off work modulation was most effective (other than simultaneously utilizing all inputs).

B. Stability Metrics

We calculated two additional stability metrics, maximum Floquet multiplier and gait sensitivity norm (Table III), and compared them with maximum tolerable disturbance. Comparisons were performed at normal walking speed using controllers designed by LQR. The maximum Floquet multipliers were obtained by measuring maximum eigenvalues of the stabilized, discrete linear model for each controller [61]. Gait sensitivity norms were calculated from 20 walking steps after an initial 0.001 m step-down disturbance, using step period as the gait indicator, in the method of [32]. As in prior studies, maximum Floquet multipliers did not correlate well with maximum tolerable disturbance (compare to Table II). Unlike prior studies, the gait sensitivity norm also did not correlate well with maximum tolerable disturbance. It may be that strong correlations observed in prior studies are limited to, e.g., 2-D models, foot-placement-based control strategies or single step-down disturbances.

C. Linearized System Model

To aid in interpreting the primary result of maximum tolerable disturbance, we performed computations based on a linearized model of the system. For this linearized model, the Poincaré section was taken at mid-stance, defined as the instant that the hip passed over the ankle ($q_{\text{ap}} = 0$). This choice eliminated the states associated with toe yaw (q_{ty}), toe pitch (q_{tp}), ankle pitch (q_{ap}), toe yaw velocity ($\dot{q}_{\text{ty}}$), and toe pitch velocity ($\dot{q}_{\text{tp}}$) from the system, since they are all typically zero at this instant. For this linearization, the model walked at normal speed. All matrices describe behavior of the system about the fixed point, relating deviations from nominal values on one step to deviations on the subsequent step. We used finite differencing to calculate the state transition matrix (Table IV), the control input matrix (Table V), and the disturbance input matrix (Table VI). To improve readability, the control input matrix was normalized. This linearized system model was used to calculate disturbance alignment and controllability.

D. Disturbance Alignment

To help interpret the reasons that push-off work control allowed better disturbance tolerance than other control inputs,

TABLE II
MAXIMUM TOLERABLE DISTURBANCE VERSUS GAIN METHOD

Control method	Measure (% leg length)	
	LQR	CMA-ES
Step width	0.96	1.10
Foot placement	1.50	1.50
Ankle roll resistance	0.12	0.78
Ankle push-off work	2.94	7.80
All inputs	3.21	7.98

TABLE III
MAXIMUM FLOQUET MULTIPLIER AND GAIT SENSITIVITY NORM

Control method	Max. Floquet multiplier	Gait sens. norm
Step width	0.513	0.093
Foot placement	0.381	0.073
Ankle roll resistance	0.533	0.114
Ankle push-off work	0.533	0.235
All inputs	0.532	0.308

TABLE IV
LINEARIZED SYSTEM: A—MID-STANCE STATE TRANSITION MATRIX

		State: x_n				
		q_{ai}	q_{hf}	$\dot{q}_{\text{ap}}$	$\dot{q}_{\text{ai}}$	$\dot{q}_{\text{hf}}$
State: x_{n+1}	q_{ai}	−2.400	0.041	0.095	−0.768	−0.006
	q_{hf}	−1.090	−0.570	0.124	−0.305	−0.022
	$\dot{q}_{\text{ap}}$	−1.690	−0.942	0.545	−0.459	−0.046
	$\dot{q}_{\text{ai}}$	−6.230	0.523	−0.296	−2.360	−0.007
	$\dot{q}_{\text{hf}}$	31.600	16.100	−3.620	8.860	0.633

TABLE V
LINEARIZED SYSTEM: B—MID-STANCE CONTROL INPUT MATRIX

		Control input: u_n				
		K_p	K_d	ϕ_{ha}	ϕ_{hf}	τ_p
State: x_{n+1}	q_{ai}	−0.154	−0.097	−0.076	0.005	−0.005
	q_{hf}	−0.022	−0.010	−0.035	0.958	−0.035
	$\dot{q}_{\text{ap}}$	−0.030	−0.020	−0.047	0.015	−0.074
	$\dot{q}_{\text{ai}}$	−0.745	−0.911	−0.193	−0.020	0.031
	$\dot{q}_{\text{hf}}$	0.648	0.399	0.976	0.286	0.996
	Norm. factor	$5.6{\cdot}10^{-4}$	$2.9{\cdot}10^{-4}$	$1.3{\cdot}10^{-1}$	$1.0{\cdot}10^{-1}$	$5.5{\cdot}10^{-1}$

TABLE VI
LINEARIZED SYSTEM: W—MID-STANCE DISTURBANCE MATRIX

		Disturbance input	
		Ht	Imp
State: x_{n+1}	q_{ai}	0.375	0.285
	q_{hf}	4.170	0.014
	$\dot{q}_{\text{ap}}$	6.370	0.066
	$\dot{q}_{\text{ai}}$	−2.310	1.260
	$\dot{q}_{\text{hf}}$	−118500	−0.473

TABLE VII
ALIGNMENT OF INPUTS AND DISTURBANCES

		Control input				
		K_p	K_d	ϕ_{ha}	ϕ_{hf}	τ_p
Dist.	Ht	0.65	0.64	0.61	0.80	1.00
	Imp	1.00	0.96	0.99	0.97	0.68

TABLE VIII
CENTER-OF-MASS STATE CONTROLLABILITY

	Control input				
	K_p	K_d	ϕ_{ha}	ϕ_{hf}	τ_p
Condition number	1382	2074	13 909	389	222

we analyzed how well the effects of each input on center-of-mass state matched those of each disturbance. For this analysis, we used the three input rows corresponding to the states primarily associated with center-of-mass position and velocity at mid-stance: q_{ai}, $\dot{q}_{\text{ap}}$, and $\dot{q}_{\text{ai}}$. This avoided confounds from states that could be strongly affected but are unlikely to lead to a fall, such as swing leg velocity at mid-stance (final swing leg position was maintained by high-gain feedback). Angle states were weighted relative to angular velocity states by the ratio of the mean standard deviation of angular velocities during a step to that of angles, which equaled 13.5. This avoided confounds due to differences in units (rad versus rad·s^{-1}). The partial input vectors were then normalized to form unit vectors (Table I). The dot product of each disturbance unit vector with each control input unit vector was calculated to determine how well-aligned inputs were with disturbances (Table VII). Push-off work (τ_p) was nearly perfectly aligned with ground-height disturbances (Ht), while the other control inputs were better aligned with lateral impulses (Imp).

E. Controllability

To help in interpreting the reasons that push-off work allowed better disturbance tolerance than other control inputs, we analyzed the ease with which each input could control center-of-mass states. We used the same techniques as for *Disturbance alignment*, using only the three states associated with center-of-mass position and velocity and weighting angle states relative to angular velocity states. We calculated the center-of-mass controllability matrix for each input, defined as $\hat{C} = [\hat{B}\ \hat{A}\cdot\hat{B}\ \hat{A}^2\cdot\hat{B}]$, where $\hat{A}$ is the (dominant) portion of the state transition matrix associated with center-of-mass states and $\hat{B}$ is the portion of the control input vector associated with center-of-mass states for each control input. We then calculated the condition number of the center-of-mass controllability matrix (Table VIII) as an indication of how easily the system could be controlled using different inputs, robustness against model errors, and the magnitude of inputs required to recover from worst-case state deviations [62]. Push-off work (τ_p) resulted in the best-conditioned center-of-mass controllability matrix, suggesting that, in general, disturbances to center-of-mass state could be removed most easily using push-off work modulation.

TABLE IX
CONTROL INPUT LINEAR RANGE

	Control input				
	K_p	K_d	ϕ_{ha}	ϕ_{hf}	τ_p
Order linear	20 $\frac{\text{N·m}}{\text{rad}}$	600 $\frac{\text{N·m·s}}{\text{rad}}$	0.04 rad	0.05 rad	700 N · m

TABLE X
DISTURBANCE TOLERANCE WITH SPRING-LIKE HIP MODEL

Control method	Measure (% leg length)	
	LQR	CMA-ES
Step width	0.04	0.13
Foot placement	0.04	0.13
Ankle roll resistance	0.17	0.28
Ankle push-off work	0.41	0.66
All inputs	0.44	0.81

F. Linearity

To aid in interpreting the finding that push-off work control resulted in the greatest disturbance tolerance, we calculated the approximate range over which control inputs had a linear effect on system state (Table IX). We iteratively recalculated each control input vector using a finite difference method, with progressively larger perturbations to the control input. We defined the linear region as the maximum perturbation for which the resulting control input matrix was within 10% of the matrix based on a small perturbation.

The linear range of push-off work was large compared to other control inputs. The maximum allowable change in push-off τ_p would result in a change of more than 350 J of mechanical work on a typical step, equivalent the change in potential energy resulting from an unexpected 0.5 m step up or down. The maximum allowable changes in ankle resistance terms K_p and K_d would result in a change of about 3 J of work on a typical step, about 1% of the value for push-off. The maximum allowable changes in foot placement terms ϕ_{ha} and ϕ_{hf} would result in a change in step width or length of about $\pm$0.05 m on a typical step, or about 28% of step width and 3.5% of step length. All control inputs other than push-off work were approximately linear up to the point at which the control input caused a fall before completion of a single walking step. Push-off work values began to have nonlinear effects prior to the values that caused a fall within one step. Push-off allowed inputs with at least one order of magnitude larger functional effect than other inputs.

G. Spring-Like Hip Control Comparison

We also compared disturbance tolerance in a model with spring-like hip actuation, equivalent to low-gain proportional control, as in [17]. We examined maximum tolerable ground-height disturbances using each high-level controller, designed using both LQR and CMA-ES methods, and found similar trends as in the model with high-gain step length control (Table X). Ankle push-off work modulation showed the best performance among individual controllers. Because gains on step length were low by definition in the spring-like hip model, once-per-step

adjustments in target step length were not very effective. Foot placement control was therefore nearly identical to step width control for the spring-like hip model.

H. Wider Step Width Model Comparison

We examined disturbance tolerance and energy expenditure for a model with larger step width (0.20 m) and compared results to the model with normal step width (0.15 m). We designed a once-per-step ankle push-off work controller using LQR for both models and compared maximum tolerable ground-height disturbance and mechanical energy expenditure. The model with wider steps walked on terrain with random height disturbances of up to 4.3% leg length, 46% higher than with nominal step width (2.9% leg length). With ground-height disturbances of 2.9% leg length, the wide step width model and nominal step width model used an average of 188.8 and 182.8 J of energy per step, respectively. As expected [63], the wide step width model therefore tolerated higher disturbances, but at a cost of more mechanical work.

I. Slope and Step-Down Disturbance Comparisons

We compared the disturbance tolerance of the foot placement and ankle roll resistance control strategies tested here to prior results to verify that they were competitive. To our knowledge no other studies have applied the same stability metrics, so we performed additional simulations using disturbances applied in other studies. We used the model with normal speed and high-gain step length control, and derived control gains using LQR. In one test, we used only foot placement control and approximated downhill walking using ten equal steps down in sequence. We found that the foot placement controller tolerated similar maximum downhill "slopes" as a prior foot placement approach (-2.5° compared to -3° slope in [53]). In a second test, we used only ankle inversion–eversion resistance control and applied a single step down. We found that this approach tolerated similar steps down as a prior approach based on center-of-pressure control (0.057 m compared to 0.025 m in [54]).

J. Maximum One-Time Lateral Impulse Comparison

We compared maximum tolerable lateral impulse, applied only once rather than randomly on each step, for three control inputs with high mediolateral control authority: push-off, step width, and inversion–eversion resistance. We used the model with normal speed and control gains derived using LQR. We incrementally increased the lateral impulse applied on the first step until the model fell within 20 walking steps. Once-per-step modulation of push-off work, step width, and inversion–eversion resistance resulted in tolerance of impulses of 0.48, 0.11, and 0.55 N·s, respectively. While inversion–eversion control resulted in the greatest one-time lateral-impulse tolerance, push-off work control resulted in comparable performance.

Acknowledgment

The authors would like to thank S. Cha for assistance in editing figures.

References

[1] W. C. Miller, A. B. Deathe, M. Speechley, and J. Koval, "The influence of falling, fear of falling and balance confidence on prosthetic mobility and social activity among individuals with a lower extremity amputation," *Arch. Phys. Med. Rehabil.*, vol. 82, no. 9, pp. 1238–1244, 2001.

[2] W. C. Miller, M. Speechley, and B. Deathe, "The prevalence and risk factors of falling and fear of falling among lower extremity amputees," *Arch. Phys. Med. Rehabil.*, vol. 82, no. 8, pp. 1031–1037, 2001.

[3] J. M. Fabre, R. Ellis, M. Kosma, and R. H. Wood, "Falls risk factors and a compendium of falls risk screening instruments," *J. Geriatric Phys. Therapy*, vol. 3932, no. 4, pp. 184–197, 2010.

[4] M. J. Major, S. Fatone, and E. J. Roth, "Validity and reliability of the berg balance scale for community-dwelling persons with lower-limb amputation," *Arch. Phys. Med. Rehabil.*, vol. 94, pp. 2194–2202, 2013.

[5] S. W. Muir, K. Berg, B. Chesworth, N. Klar, and M. Speechley, "Balance impairment as a risk factor for falls in community-dwelling older adults who are high functioning: A prospective study," *Phys. Ther.*, vol. 90, pp. 338–347, 2010.

[6] S. W. Muir, K. Berg, B. Chesworth, N. Klar, and M. Speechley, "Quantifying the magnitude of risk for balance impairment on falls in community-dwelling older adults: A systematic review and meta-analysis," *J. Clin. Epidemiol.*, vol. 63, pp. 389–406, 2010.

[7] A. Esquenazi and R. DiGiacomo, "Rehabilitation after amputation," *J. Amer. Podiatric Med. Assoc.*, vol. 91, no. 1, pp. 13–22, 2001.

[8] J. R. Crenshaw, K. R. Kaufman, and M. D. Grabiner, "Compensatory-step training of healthy, mobile people with unilateral, transfemoral or knee disarticulation amputations: A potential intervention for trip-related falls," *Gait Posture*, vol. 38, no. 3, pp. 500–506, 2013.

[9] J. R. Crenshaw, K. R. Kaufman, and M. D. Grabiner, "Trip recoveries of people with unilateral, transfemoral or knee disarticulation amputations: Initial findings," *Gait Posture*, vol. 38, pp. 534–536, 2013.

[10] H. M. Herr and A. M. Grabowski, "Bionic ankle-foot prosthesis normalizes walking gait for persons with leg amputation," *Proc. Roy. Soc. London B, Biol. Sci.*, vol. 279, pp. 457–464, 2012.

[11] M. Goldfarb, B. E. Lawson, and A. H. Schultz, "Realizing the promise of robotic leg prostheses," *Sci. Transl. Med.*, vol. 5, no. 210, pp. 1–6, 2013.

[12] J. Hitt, T. Sugar, M. Holgate, R. Bellman, and K. Hollander, "Robotic transtibital prosthesis with biomechanical energy regeneration," *Ind. Robot, Int. J.*, vol. 36, no. 5, pp. 441–447, 2009.

[13] J. M. Caputo and S. H. Collins, "A universal ankle-foot prosthesis emulator for experiments during human locomotion," *ASME J. Biomech. Eng.*, vol. 136, 2014, Art. no. 035002.

[14] J. M. Aldridge, J. T. Sturdy, and J. M. Wilken, "Stair ascent kinematics and kinetics with a powered lower leg system following transtibial amputation," *Gait Posture*, vol. 36, no. 2, pp. 291–295, 2012.

[15] D. H. Gates, S. J. Scott, J. M. Wilken, and J. B. Dingwell, "Frontal plane dynamic margins of stability in individuals with and without transtibial amputation walking on a loose rock surface," vol. 38, no. 4, pp. 570–575, 2013.

[16] B. E. Lawson, H. A. Varol, A. Huff, E. Erdemir, and M. Goldfarb, "Control of stair ascent and descent with a powered transfemoral prosthesis," *IEEE Trans. Neural Syst. Rehabil. Eng.*, vol. 21, no. 3, pp. 466–473, May 2013.

[17] A. D. Kuo, "Stabilization of lateral motion in passive dynamic walking," *Int. J. Robot. Res.*, vol. 18, no. 9, pp. 917–930, 1999.

[18] J. Pratt, J. Carff, S. Drakunov, and A. Goswami, "Capture point: A step toward humanoid push recovery," in *Proc. IEEE-RAS Int. Conf. Humanoid Robots*, 2006, pp. 200–207.

[19] S. M. O'Connor, H. Z. Xu, and A. D. Kuo, "Energetic cost of walking with increased step variability," *Gait Posture*, vol. 36, no. 1, pp. 102–107, 2012.

[20] S. H. Collins and A. D. Kuo, "Two independent contributions to step variability during over-ground human walking," *Public Library Sci., ONE*, vol. 8, no. 8, 2013, Art. no. e73597.

[21] J.-Y. Kim, I.-W. Park, and J.-H. Oh, "Walking control algorithm of biped humanoid robot on uneven and inclined floor," *J. Intell. Robot. Syst.*, vol. 48, no. 4, pp. 457–484, 2007.

[22] A. L. Hof, S. M. Vermerris, and W. A. Gjaltema, "Balance responses to lateral perturbations in human treadmill walking," *J. Exp. Biol.*, vol. 213, no. 15, pp. 2655–2664, 2010.

[23] A. L. Hof, R. M. van Bockel, T. Schoppen, and K. Postema, "Control of lateral balance in walking: Experimental findings in normal subjects and above-knee amputees," *Gait Posture*, vol. 25, pp. 250–258, 2007.

[24] A. Ruina, J. E. A. Bertram, and M. Srinivasan, "A collision model of the energetic cost of support work qualitatively explains leg sequencing in walking and galloping, pseudo-elastic leg behavior in running and the walk-to-run transition," vol. 237, pp. 170–192, 2005.

[25] P. A. Bhounsule *et al.*, "Low-bandwidth reflex-based control for lower power walking: 65 km on a single battery charge," *Int. J. Robot. Res.*, vol. 33, no. 10, pp. 1305–1321, 2014.
[26] D. G. E. Hobbelen and M. Wisse, "Ankle actuation for limit cycle walkers," *Int. J. Robot. Res.*, vol. 27, no. 6, pp. 709–735, 2008.
[27] A. D. Kuo, J. M. Donelan, and A. Ruina, "Energetic consequences of walking like an inverted pendulum: Step-to-step transitions," *Exercise Sport Sci. Rev.*, vol. 33, pp. 88–97, 2005.
[28] A. E. Martin, D. C. Post, and J. P. Schmiedeler, "The effects of foot geometric properties on the gait of planar bipeds walking under HZD-based control," *Int. J. Robot. Res.*, vol. 33, no. 12, pp. 1530–1543, 2014.
[29] M. M. van der Krogt, D. J. J. Bregman, M. Wisse, C. A. M. Doorenbosch, J. Harlaar, and S. H. Collins, "How crouch gait can dynamically induce stiff-knee gait," *Ann. Biomed. Eng.*, vol. 38, pp. 1593–1606, 2010.
[30] J. M. Donelan, D. W. Shipman, R. Kram, and A. D. Kuo, "Mechanical and metabolic requirements for active lateral stabilization in human walking," *J. Biomech.*, vol. 37, no. 6, pp. 827–835, 2004.
[31] S. M. Bruijn, O. G. Meijer, P. J. Beek, and J. H. V. Dieën, "Assessing the stability of human locomotion: A review of current measures," *J. Roy. Soc. London, Interface*, vol. 10, no. 83, 2013, Art. no. 20120999.
[32] D. G. E. Hobbelen and M. Wisse, "A disturbance rejection measure for limit cycle walkers: The gait sensitivity norm," *IEEE Trans. Robot.*, vol. 23, no. 6, pp. 1213–1224, Dec. 2007.
[33] S. Song, C. LaMontagna, S. H. Collins, and H. Geyer, "The effect of foot compliance encoded in the windlass mechanism on the energetics of human walking," in *Proc. IEEE Int. Conf. Eng. Med. Biol. Soc.*, 2013, pp. 3179–3182.
[34] T. Krasovsky, A. Lamontagne, A. G. Feldman, and M. F. Levin, "Effects of walking speed on gait stability and interlimb coordination in younger and older adults," *Gait Posture*, vol. 39, no. 1, pp. 378–385, 2014.
[35] D. D. Espy, F. Yang, T. Bhatt, and Y.-C. Pai, "Independent influence of gait speed and step length on stability and fall risk," *Gait Posture*, vol. 32, no. 3, pp. 378–382, 2010.
[36] N. Kadono and M. J. Pavol, "Effects of aging-related losses in strength on the ability to recover from a backward balance loss," *J. Biomech.*, vol. 46, no. 1, pp. 13–18, 2013.
[37] T. Ijmker *et al.*, "Effect of balance support on the energy cost of walking after stroke," *Arch. Phys. Med. Rehabil.*, vol. 94, no. 11, pp. 2255–2261, 2013.
[38] A. S. Voloshina, A. D. Kuo, M. A. Daley, and D. P. Ferris, "Biomechanics and energetics of walking on uneven terrain," *J. Exp. Biol.*, vol. 216, pp. 3963–3970, 2013.
[39] A. Sala and A. Esparza, "Reduced-order controller design via iterative identification and control," *Eur. J. Control*, vol. 9, no. 1, pp. 105–117, 2003.
[40] J. M. Zurada, "Sensitivity analysis for minimization of input data dimension for feedforward neural network," *Circuits Syst.*, vol. 6, pp. 447–450, 1994.
[41] M. Kim and S. H. Collins, "Stabilization of a three-dimensional limit cycle walking model through step-to-step ankle control," in *Proc. IEEE Int. Conf. Rehabil. Robot.*, 2013, pp. 1–6.
[42] D. A. Winter, *The Biomechanics and Motor Control of Human Gait: Normal, Elderly and Pathological*. Waterloo, ON, Canada: Waterloo Biomech., 1991.
[43] R. Chandler, C. Clauser, J. McConville, H. Reynolds, and J. Young, "Investigation of inertial properties of the human body," Air Force Aerosp. Med. Res. Lab Wright-Patterson AFB OH, Washington, DC, USA, Tech. Rep. no. AMRL-TR-74-137, 1975.
[44] A. D. Kuo, "The dynamics workbench," 2012. [Online]. Available: http://www-personal.umich.edu/~artkuo/DynamicsWorkbench/
[45] M. J. Hsu, D. H. Nielsen, S. J. Lin-Chan, and D. Shurr, "The effects of prosthetic foot design on physiologic measurements, self-selected walking velocity, and physical activity in people with transtibial amputation," *Arch. Phys. Med. Rehabil.*, vol. 87, pp. 123–129, 2006.
[46] S. H. Collins, P. G. Adamczyk, and A. D. Kuo, "Dynamic arm swinging in human walking," *Proc. Roy. Soc. London B, Biol. Sci.*, vol. 276, pp. 3679–3688, 2009.
[47] M. Wisse, A. L. Schwab, R. Q. van der Linde, and F. C. T. van der Helm, "How to keep from falling forward: Elementary swing leg action for passive dynamic walkers," *IEEE Trans. Robot.*, vol. 21, no. 3, pp. 393–401, Jun. 2005.
[48] J. M. Caputo and S. H. Collins, "Prosthetic ankle push-off work reduces metabolic rate but not collision work in non-amputee walking," *Nature Sci. Rep.*, vol. 4, 2014, Art. no. 7213.
[49] N. Hansen, "The CMA evolution strategy: A comparing review," in *Towards a New Evolutionary Computation*, J. A. Lozano, Ed. Berlin, Germany: Springer, 2006, pp. 75–102.
[50] S. H. Collins, A. Ruina, R. Tedrake, and M. Wisse, "Efficient bipedal robots based on passive-dynamic walkers," *Science*, vol. 307, pp. 1082–1085, 2005.
[51] S. H. Collins, M. B. Wiggin, and G. S. Sawicki, "Reducing the energy cost of human walking using an unpowered exoskeleton," *Nature*, vol. 522, pp. 212–215, 2015.
[52] A. D. Kuo, "A simple model predicts the step length-speed relationship in human walking," *ASME J. Biomech. Eng.*, vol. 123, pp. 264–269, 2001.
[53] J. M. Wang, D. J. Fleet, and A. Hertzmann, "Optimizing walking controllers," *ACM Trans. Graph.*, vol. 28, no. 5, 2009, Art. no. 168.
[54] S. Kajita and K. Tan, "Study of dynamic biped locomotion on rugged terrain-derivation and application of the linear inverted pendulum model," in *Proc. IEEE Int. Conf. Robot. Autom.*, 1991, pp. 1405–1411.
[55] R. Tedrake, I. R. Manchester, M. Tobenkin, and J. W. Roberts, "LQR-trees: Feedback motion planning via sums-of-squares verification," *Int. J. Robot. Res.*, vol. 29, no. 8, pp. 1038–1052, 2010.
[56] M. Benallegue, J.-P. Laumond, and A. Berthoz, "Contribution of actuated head and trunk to passive walkers stabilization," in *Proc. IEEE Int. Conf. Robot. Autom.*, 2013, pp. 5638–5643.
[57] S. M. Bruijn, O. G. Meijer, P. J. Beek, and J. H. van Dieën, "The effects of arm swing on human gait stability," *J. Exp. Biol.*, vol. 213, pp. 3945–3952, 2010.
[58] S. Kuindersma *et al.*, "Optimization-based locomotion planning, estimation, and control design for the atlas humanoid robot," *Auton. Robots*, vol. 40, no. 3, pp. 429–455, 2016.
[59] S. Feng, "Online hierarchical optimization for humanoid control," Ph.D. dissertation, Robot. Inst., Carnegie Mellon Univ., Pittsburgh, PA, USA, 2016.
[60] M. Kim and S. H. Collins, "Once-per-step control of ankle-foot prosthesis push-off work reduces effort associated with balance during human walking," *J. NeuroEng. Rehabil.*, vol. 12, 2015, Art. no. 43.
[61] T. McGeer, "Passive dynamic walking," *Int. J. Robot. Res.*, vol. 9, pp. 62–82, 1990.
[62] K. Zhou and J. C. Doyle, *Essentials of Robust Control*. Englewood Cliffs, NJ, USA: Prentice Hall, 1997.
[63] J. M. Donelan, R. Kram, and A. D. Kuo, "Mechanical and metabolic determinants of the preferred step width in human walking," *Proc. Roy. Soc. London B, Biol. Sci.*, vol. 268, pp. 1985–1992, 2001.
[64] J. Towns *et al.*, "XSEDE: Accelerating scientific discovery," *Comput. Sci. Eng.*, vol. 16, no. 5, pp. 62–74, 2014.

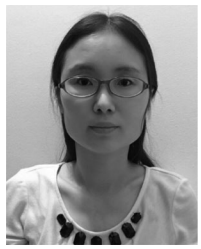

Myunghee Kim received the B.S. degree from Hayang University, Seoul, South Korea, in 2002; M.S. degree from Korea Advanced Institute of Science and Technology, Daejeon, South Korea, in 2004 and from Massachusetts Institute of Technology, Cambridge, MA, USA, in 2006; and the Ph.D. degree from Carnegie Mellon University, Pittsburgh, PA, USA, in 2015, all in mechanical engineering.

She was a Control Engineer in humanoid robotics at Samsung. She currently is a Postdoctoral Fellow with Wyss Institute for Biologically Inspired Engineering, and in the School of Engineering and Applied Sciences, Harvard University, Cambridge, MA, USA. Her research focus is on designing individualized controllers to reduce walking efforts including balance.

Dr. Kim received the Best Paper Award in the medical devices category at ICRA 2015.

Steven H. Collins received the B.S. degree from Cornell University, Ithaca, NY, USA, in 2002 and the Ph.D. degree from University of Michigan, Ann Arbor, MI, USA, in 2008, both in mechanical engineering.

He was a Postdoctoral Researcher at TU Delft, Delft, The Netherlands. He is an Associate Professor of mechanical engineering with Carnegie Mellon University, Pittsburgh, PA, USA, where he directs the Experimental Biomechatronics Laboratory and teaches courses on design and biomechatronics. He is a member of the Scientific Board of Dynamic Walking. His research addresses tools to speed and systematize development of prostheses and exoskeletons, experiments to discover and characterize new assistance techniques, and translation to high-efficiency mobile assistive devices.

Dr. Collins received the ASB Young Scientist Award and was recently voted Mechanical Engineering Professor of the Year.